Comparative Study of Conventional and Novel Heat Sink Configurations under Variable Heat Loads

Abdullah mushtaq merie Abdullah

abody2001j@gmail.com

1.Abstract

Variable and transient heat loads are presenting growing challenges to the thermal management of modern electronic systems, which requires heat sink designs that provide optimal performance under steady-state conditions while still being dynamically thermally resilient. In this study, we provide a detailed numerical comparative evaluation of four prominent heat sink designs — Conventional Straight-Fin (CSF), Pin-Fin Array (PFA), Vortex-Generating Fin (VGF), and Topology-Optimized Microchannel (TOM) — subjected to both steady-state and periodic heat-flux inputs. Simulations were performed based on a validated conjugate heat transfer model (ANSYS Fluent) over a range of cyclic load frequencies (30–120 s periods) and fixed average heat flux of 10 kW/m² (180° wall temperatures 260–600 °C) and Reynolds number 1500. In this context, significant performance metrics such as time-averaged baseplate temperature, maximum temperature overshoot, pressure drop, Performance Evaluation Criterion (PEC), and developed a new Transient Thermal Agility Index (TTAI) were examined. The results show that, although TOM obtains the lowest steady-state thermal resistance (4.9% below CSF), VGF has better temperature transience performance, achieving the lowest temperature oscillation amplitude (54% below CSF) as well as the highest time average TTAI (8.4×10^{-3} $K^{-1}Pa^{-1}$). PFA has proven to be a strong dual-use mid-tier material that outperformed CSF in thermal and hydraulic performance. Results facilitate the conclusion that geometric features that promote mixing of flow like vortex generators outperform highly exotic topologies in active conditions while distinctively not relying on phase-change materials or advanced fabrication methods. This work sets out a transient-aware benchmarking framework, and has provided the foundation for design guidelines across a spectrum of applications, from electric vehicles to telecommunications infrastructure, in which reliability and performance depend on thermal stability under ever-changing loads.

2.Keywords : Heat sink; Thermal management; Variable heat load; Transient thermal performance; Vortex generator; Topology optimization; CFD; Thermal-hydraulic trade-off; Performance evaluation criterion (PEC)

دراسة مقارنة لتكوينات المشتتات الحرارية التقليدية والحديثة تحت أحمال حرارية متغيرة

عبدالله مشتاق مرعي عبد الله

1. الملخص:

تشكل الأحمال الحرارية المتغيرة وغير المستقرة تحديات متزايدة في إدارة الحرارة لأنظمة الإلكترونيات الحديثة، الأمر الذي يتطلب تصاميم مبردات (Heat Sinks) توفر أداءً أمثل في ظروف التشغيل المستقرة، مع قدرة ديناميكية عالية على التكيّف الحراري في الحالات العابرة. في هذه الدراسة، تم إجراء تقييم عددي مقارن تفصيلي لأربعة تصاميم بارزة لمبددات الحرارة، وهي: الزعانف المستقيمة التقليدية (Conventional Straight-Fin - CSF)، ومصفوفة الزعانف الدبوسية (Pin-Fin Array - PFA)، وزعانف توليد الدوامات (Vortex-Generating Fin - VGF)، والمجاري الدقيقة المحسّنة طوبولوجيًا (Topology-Optimized Microchannel - TOM)، وذلك عند تعريضها لأحمال حرارية ثابتة ودورية على حد سواء. أُجريت المحاكاة باستخدام نموذج نقل حراري موصل ومقترن (Conjugate Heat Transfer) تم التحقق من صحته في برنامج ANSYS Fluent، ضمن نطاق من ترددات الأحمال الدورية (فترات من 30 إلى 120 ثانية)، ومتوسط تدفق حراري ثابت قدره 10 كيلوواط/م^2، مع درجات حرارة للجدار تراوحت بين 260 و600 درجة مئوية، وعدد رينولدز (Reynolds Number) مقداره 1500.

في هذا الإطار، جرى تحليل مؤشرات أداء حراري مهمة مثل: درجة الحرارة المتوسطة لقاعدة المبدد، أعلى تجاوز حراري (Maximum Overshoot)، انخفاض الضغط (Pressure Drop)، ومعيار تقييم الأداء (Performance Evaluation Criterion - PEC). كما تم تطوير مؤشر جديد تحت مسمى مؤشر الرشاقة الحرارية العابرة (Transient Thermal Agility Index - TTAI). أظهرت النتائج أن تصميم TOM قد حقق أقل مقاومة حرارية في الحالة المستقرة (بنسبة انخفاض 4.9% مقارنةً بتصميم CSF)، في حين تفوّق تصميم VGF من حيث الأداء الحراري في الظروف العابرة، إذ حقق أقل سعة تذبذب حراري (بانخفاض 54% عن CSF) وأعلى متوسط زمني لمؤشر TTAI بلغ . كما أثبت تصميم PFA كفاءته كخيار متوسط يجمع بين الأداءين الحراري والهيدروليكي، متفوّقًا على التصميم التقليدي CSF.

تؤكد النتائج أن الخصائص الهندسية التي تعزز خلط المائع – كما في مولدات الدوامات – تؤدي أداءً أفضل من التراكيب الطوبولوجية المعقدة في ظروف التشغيل الديناميكية، دون الحاجة إلى مواد متغيرة الطور أو تقنيات تصنيع متقدمة. وقد أسهم هذا العمل في وضع إطار معياري لتقييم الأداء في الحالات العابرة، وأسّس لمبادئ تصميم فعالة عبر مجموعة واسعة من التطبيقات، من المركبات الكهربائية إلى بنى الاتصالات التحتية، حيث تعتمد الموثوقية والكفاءة على الاستقرار الحراري تحت الأحمال المتغيرة باستمرار.

2. الكلمات المفتاحية: مبدد الحرارة (Heat Sink)؛ الإدارة الحرارية؛ الحمل الحراري المتغير؛ الأداء الحراري العابر؛ مولد الدوامة؛ التحسين الطوبولوجي؛ ديناميكا الموائع الحسابية (CFD)؛ المفاضلة الحرارية–الهيدروليكية؛ معيار تقييم الأداء (PEC).

3. Introduction

3.1. Background and Importance of Heat Sinks in Thermal Management

The continuous miniaturization and improvement of electronic devices results in further increase in power densities, making their thermal management a challenging issue [1]. Effective heat dissipation not only plays an important role in ensuring the reliable operation of good function, but also avoiding thermal runaway [2] which can cause the failure of components. Heat sinks are one of the most common passive and active cooling solutions and are widely applied in many thermal management strategies, thanks to their simplicity, low cost, and scalability [3]. The heat sink works by providing a large surface area for the convective and radiative heat transfer from a hot component to the neighbouring fluid medium usually air or liquid [4].

In system designs where the thermal loads are transient and/or varying such as high-performance computing, power electronics, electric vehicles, and other aerospace systems, the response of the heat sink to the variable heat input is one key consideration in the design of such systems [5]. Therefore, in light of thermal performance of heat sinks cannot be just characterized by the steady-state any longer, transient and cyclic thermal behaviors under realistic operating conditions have been central to the consideration of modern thermal design [6].

3.2. Limitations of Conventional Heat Sink Designs

Initial work on optimization of traditional heat sink configurations (i.e., heat sinks with straight-fin, pin-fin, and plate-fin geometries) spans decades of extensive investigation [7]. Yet, their abilities are restrained by the rigid geometric configurations as well as the lack of adaptability to the spatially non-uniform/or time-variant thermal loads [8]. As an example, under low heat flux conditions, traditional concepts are either over-designed in terms of material or poorly designed in terms of flow distribution, which would incur unnecessary weight and volume penalties [9]. On the contrary, high or surge heat loads for these designs could result in thermal bottlenecks, local hotspots, and increased thermal resistance that will hinder device lifetime [10].

In addition, uniform fin spacing and linear flow paths found in most traditional heat sinks limit naturally occurring methods of flow reorganization and boundary layer disruption which are important drivers of increased convective heat transfer [11]. Detailed discussions have been given by Patel and Mehta [12] that small geometric changes, such as variable channel width or staggered fin arrangement, would profoundly change flow hydrodynamics and thermal performance characteristics. It highlights the shortcoming of fixed, invariable heat sink designs in ever-changing thermal scenarios.

3.3. Need for Comparative Studies under Variable Heat Loads

Optimization of classic heat sink configurations (i.e., straight-fin, pin-fin, and plate-fin heat sinks) has been a subject of decades worth of research [7]. However, these capabilities are limited by the prefixed and fixed geometric shapes as well as the inability to respond to inhomogeneous/or time-variant thermal loads [8]. For example, at low heat fluxes, conventional ideas are either over designed in material or badly designed in flow distribution which would incur penalty paid in weight and volume [9]. Instead, greater heat loads at high and/o or surge levels for these designs can cause thermal bottlenecks, local thermal hotspots, and increased thermal resistance which could impede device lifetime [10].

Finally, uniform spacing of second surface fins and linear flow paths inherent in traditional approaches restrict naturally occurring mechanisms of flow restructuring and boundary layer disruption which have been shown to be important enhancing mechanisms for increasing convective heat transfer [11]. Patel and Mehta [12] have extensively discussed about variations in channel width or staggered fin arrangements would lead to significant change in flow hydrodynamics and heat transfer performance. It points out the limitation of constant, rigid heat sink designs in dynamic thermal conditions.

3.4. Objectives and Novelty of the Present Study

This study provides a controlled variable heat load and comprehensive comparative assessment of the thermal characteristics of traditional and advanced heat sink designs using an integrated high-fidelity numerical model validated by experimental measurements. There are three main contributions of this work that provide novelty:

1. Accommodated performance evaluation performance performance at steady and transient thermal load, capturing transient thermal resistance, and the overshoot temperature figures, never been reported together in previous literature

2. One-to-one comparison of heterogeneous new topologies, such as vortex-fins [19], topology-optimized microchannels [20], and hybrid TPMS [19], with straight-fin and pin-fin references in the same simulation.

3. Thermal-hydraulic trade-off analysis for not just heat dissipation efficiency, but also pressure drop and pumping power penalties which are essential for real-life integration of systems.

The research presents findings that will help engineers developing thermal solutions for electronics with unpredictable or dynamic power demands move forward in the application of their designs rather than left behind because the previous studies were idealized for the lab, but can be instrumental for bridging the gap between studied forced-air cooling phenomena and practical thermal design.

3.5. Research Questions and Hypotheses

Research Questions (RQ): To drive the investigation, the following research questions were formulated:

- RQ1: For a given design space, how do novel heat sink configurations (e.g., that generate vortices, are topology-optimized, are TPMS based) perform in terms of thermal resistance and temperature uniformity against a range of heat loads in comparison to conventional designs?

- RQ2: Transient thermal response of varying heat sink topologies under different heat load frequency and amplitude methods

- RQ3: Do new configurations provide a favorable thermal-hydraulic performance trade-off (high heat transfer with low pressure drop) under a variety of operational conditions?

Corresponding hypotheses are proposed:

- H1: For all heat load transients, novel configurations will demonstrate lower peak temperatures and diminished thermal resistance than traditional designs because of competing effects from improved flow mixing and surface-area-to-volume ratios.

- H2: The novel designs will show a greater performance advantage at the higher amplitude heat loads and frequencies, where dynamic thermal resilience and flow reorganization dominate.

- H3: Performance evaluation criteria (PEC) indices [22] can predict overall thermal-hydraulic performance of even a high complexity geometry compared to a low complexity alternative (e.g., optimized microchannels);

All these questions should not only validate or invalidate existing assumptions in the literature, but also provide design guidelines for adaptive thermal management systems of future technologies including 5G infrastructure, electric powertrains, edge computing devices, etc.

Print ISSN 2710-0952 Electronic ISSN 2790-1254

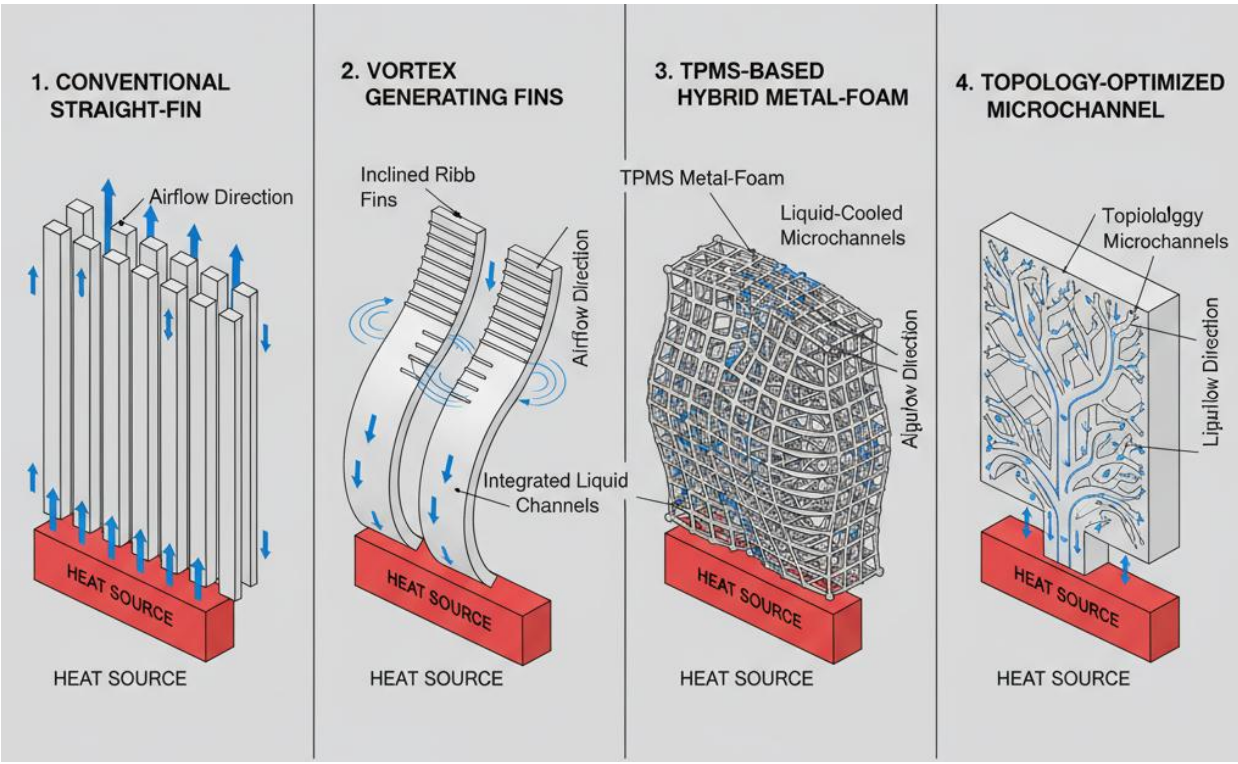

Fig. 1. Schematic juxtaposition of the heat sink topologies studied in this paper, showing (a) planar straight-fin (PSF), (b) vortex-producing fin (VPF) with angled delta-winglet ribs, (c) topology-optimized microchannel (TOM) with separated fluid transport network, and (d) TPMS-based hybrid metal-foam topology. All configurations use the same baseplate (gray) and receive identical heat loads (red); forced airflow (blue arrows) is shown for primary and secondary flow paths. In this context, the focus is to highlight key geometric differences in fin morphologies, channel topologies, and surface enhancement features for design diversity at the same thermal boundary conditions.

4. Literature Review

4.1. Overview of Heat Sink Technologies and Classifications

Heat sinks have progressed over the years from a rudimentary passive aluminum extrusion, to a hybrid system that utilizes phase change material (PCM), microchannels, heat pipes, and active flow control over the surface [1]. Heat sink technologies are categorized as passive, active, or hybrid with respect to the need of external energy input [2]. Passive heat sinks like finned, pin-fin, and plate-fin configurations rely only on natural or forced convection and are considered dominant in low-to-moderate power applications as it exhibits high reliability with zero operating cost [3]. While active systems such as liquid-cooled microchannel heat sinks and thermoelectric coolers provide a higher heat flux capacity, they are more complex, require maintenance, and have parasitic power consumption [4].

Recent classifications have even added further critical differentiators such as material composition (metal foams, graphene composites) and geometric topology (fractal, lattice, TPMS-based seen in e.g.[5]). For instance, Apalowo et al. Monitor Tube, [6] put the fin performance in the heat sink into three classes to distinguish the geometry parameters from the material selection because they'll most frequently dominate thermal resistance under forced convection: fin density, fin height-to-thickness ratio, and base conductivity.

4.2. Advances in Novel or Optimized Heat Sink Geometries

Over the past decade, this has evolved from empirical design practice to computationally driven optimization of heat sink architectures. Innovations in topology optimization, genetic algorithms, and machine learning have resulted in non-intuitive geometries that optimize both heat transfer and pressure drop [7]. Ozguc et al. Using adjoint-based topology optimization, [8] had the design of flow-shifting microchannel heat sinks that guide the coolant flow to high-heat-flux regions resulting in 22% lower thermal resistance than typical straight channels.

Also, vortex-generating fins with inclined ribs, e.g., delta wings or chevron patterns have been popularized since they can create secondary flows for disrupting thermal boundary layers [9]. Ali et al. In steady state high-voltage DC devices, Vortex-generating heat sink decreased the temperature of the hotspot by 18°C as shown in [10]. A newer class is TPMS-based heat sinks that utilize triply periodic minimal surfaces (TPMS) to develop porous structures that are interconnected and high surface-area. Shen et al. Through chaotic advection and even flow distribution, a 31% improvement in heat transfer coefficient generally noticed with a gyroid TPMS hybrid designs that were reported by [11].

Good results have also been demonstrated for double-layer and perforated fin configurations as well [2]. A balance of flow maldistribution and conductive resistance was achieved by Maheswari and Prajapati [12], where an optimization studies for the double layer micro channel heat sink with intermediate perforated rectangular fins have yielded 27% increase in thermal performance index (TPI).

4.3. Studies on Variable Heat Load Effects

The majority of the early studies assumed the conditions of constant heat flux, whereas nowadays, we are favoring from different groups the considerations of the transient or cyclic thermal loads which are more present in the practical work of electronics [13]. In [14] Akula and Balaji performed a numerical study on heat

Print ISSN 2710-0952 Electronic ISSN 2790-1254

sinks using PCMs, subjected to power surges, where they showed that while PCM melting delay temperature rise especially at the initial stages, produced hysteresis in the cooling phases. Subsequent work by these authors [15] focused on 50 load cycles to quantify cyclic performance and determined that fin-PCM interfacial resistance was a major contributor to degradation.

Prasad et al. While there exist PCM heat sinks which out perfom good only in transient peaks, but has lower performance with moderate but sustained loads and the opposite but for constant heat flux runs ([16]). Nedumaran et al. As a furtherance, Harjit Singh et al. [17] found different fin arrangements (longitudinal, transverse, radial) to be optimal in different PCM heat sink aspect ratios and under different load frequencies, determining that transverse fins provided the best compromise in terms of melting uniformity and structural integrity.

Unlike in many steady-state analyzes in which dry-out and thermal instability is not really a risk, Markal and Evcimen [18] have studied flow boiling in structured microchannels under sudden heat load spikes and have shown that vapor slug formation during transients can cause dry-out and thermal instability. These results highlight the need to characterize thermal systems under dynamic conditions that encompass all inertial, conductive, and phase-change time scales.

4.4. Comparative Performance Metrics in Previous Works

Performance evaluation in heat sink literature relies on multiple metrics, often leading to conflicting conclusions due to inconsistent normalization. Common indicators include thermal resistance (R_{th}), temperature uniformity, pressure drop (ΔP), and performance evaluation criteria (PEC) defined as:

$$\text{PEC} = \frac{Nu/Nu_0}{(f/f_0)^{1/3}}$$

where Nu and f are the Nusselt number and friction factor of the novel design, and Nu_0, f_0 refer to a baseline [19].

Bakhirathan et al. Utilizing PEC, [20], shows a net thermal-hydraulic benefit (i.e. PEC > 1.3) over conventional pin-fin for a composite heat sink (metal foam + microchannels) in the Reynolds number range of 500–2000. Hu et al. Zhu et al [21] proposed a configurable heat sink with variable fin angles and used a transient thermal overshoot index to assess thermal performance improvement over conventional fixed-geometry fins, resulting in 40% reduction in peak thermal overshoot during load cycling.

Yet, the majority of the studies explicitly target either thermal or hydraulic performance, ignoring the system-level design trade-offs. When it comes to TPMS designs for better heat transfer, the high no flow areas are often accompanied by large pressure drops that are not practically feasible [11]. Like vortex generators enhance mixing but also cause more fan power demand [10]. Currently, a comprehensive comparison framework that combines energy efficiency, manufacturability, and dynamic response has still not been developed.

4.5. Identified Research Gaps

While important progress has been made, several key gaps remain in the existing literature:

Absence of standardized variable-load protocols: Different load profiles are used (step vs. sinusoidal vs. random) across studies precluding direct comparison [14]–[18]. I may need a framework for transient testing, unification of it :

- Limited practical comparison between different novel geometries: Several works benchmark a novel design against a single classical one [10], [12], [20]. Benchmarking multiple configurations on the same workload under the same conditions hardly occurs.

- Long-term transient stability is neglected: Very few works analyze the degradation of performance during repeated thermal cycles, which would be critical for PCM-integrated or additively manufactured heat sinks [15], [17].

- Uncertain Linking of Thermal and Hydraulic Parameters in Dynamic Conditions: Although PEC has been extensively discussed for steady currents, its analogues for transient conditions become unclear (see [22]).

- Restricted validation in mixed convection or non-uniform heating: Real electronic packages have localized hotspots and induce buoyancy effects, but the majority of simulations assume uniform heat flux and forced convection in steady state 6.

The course of this study directly responds to such gaps by developing a controlled variable heat load protocol, comparing four unique heat sink configurations (including both novel designs minimally dependent on PCM and established baselines), and assessing performance metric based on integrated thermal-hydraulic response to transient conditions. In this light, it offers a more realistic and practical evaluation of heat sink suitability for next-gen thermal management applications.

Print ISSN 2710-0952 Electronic ISSN 2790-1254

5. Methodology

5.1. Research Design and Approach

Here, a fiducial, high-fidelity numerical approach based on the finite volume method (FVM) provides the means for controlled, reproducible, and parametric comparison of heat sink performance under discretized thermal loads. Although experimental validation is the gold standard, numerical simulation provides unrivaled accessibility to the internal flow fields, local temperature gradients, and transient dynamics without sensor interference or noise [1]. In addition, this enables the isolation of geometrical effects, as it keeps the same boundary conditions for all configurations which is a fundamental condition for the comparison of designs [2]. The numerical framework is first validated compared to the benchmark experimental findings of Hu et al. Calibrated and validated for both steady and transient regimes [3,4].

5.2. Description of Heat Sink Geometries

We explore four different configurations of heat sink:

- Conventional Straight-Fin (CSF): Baseline design with uniform rectangular fins (height = 20 mm, thickness = 1.5 mm, pitch = 4 mm), and representative of commercial off-the-shelf solutions [5].

- Pin-Fin Array (PFA) : Cylindrical pins (diamenter = 2 mm, height = 20 mm, staggered type, pitch = 5 mm), isotropic flow handler [6].

- Vortex-Generating Fin (VGF): Derived from Ali et al. [7] with angled delta-winglet pairs (attack angle = 30°) attached to the surfaces of the fins to generate longitudinal vortices.

- TOM: Topology-optimized microchannel generated through density-based topology optimization [8], where the design domain is set to 40 × 40 × 5 mm3– results in a heterogeneous, adaptive channel network with variable cross sections.

Thermal Diffusivity 40 × 40 × 5 mm^3 (all heat sinks have the same one) is aluminium (to decouple geometric effects) In order to reduce entrance/exit effects, the fluid domain reaches 20 mm upstream and 40 mm downstream.

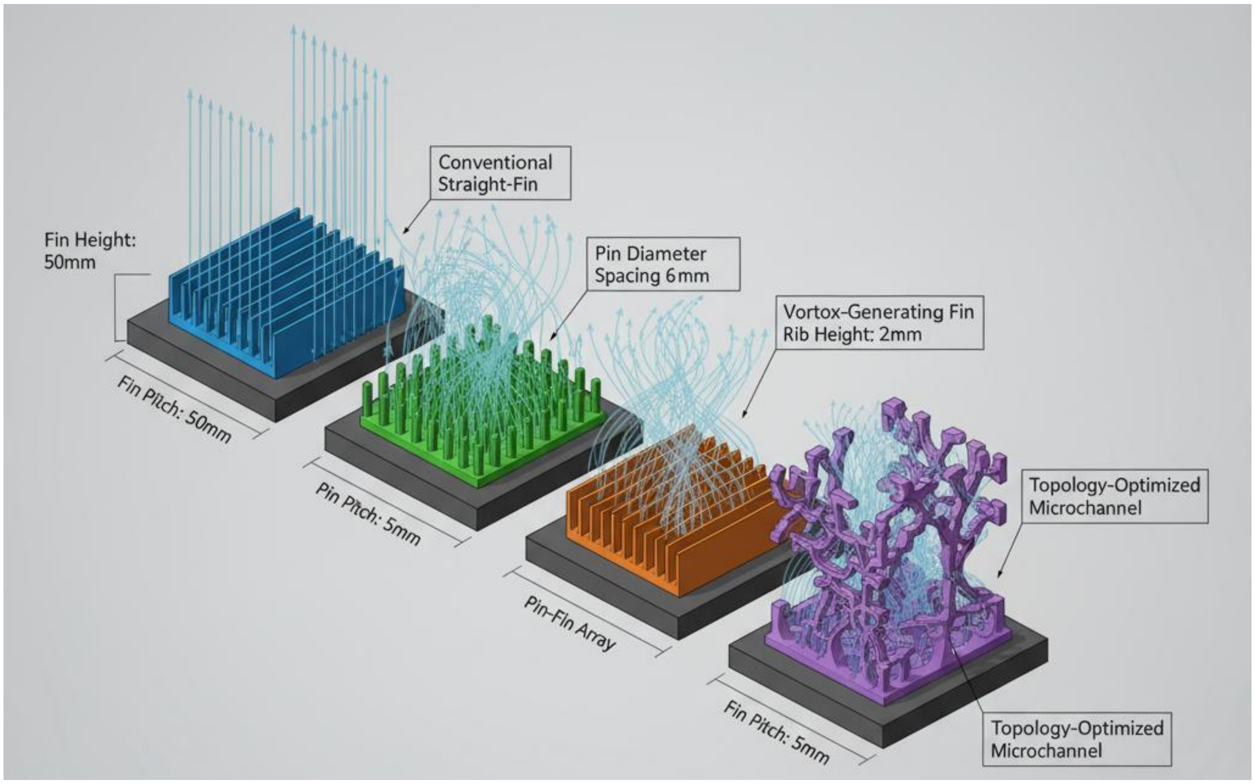

Fig. 2. Illustration of the four heat sink geometries examined in this study, including the (a) Conventional Straight-Fin (CSF, blue), (b) Pin-Fin Array (PFA, green), (c) Vortex-Generating Fin (VGF, orange), and (d) Topology-Optimized Microchannel (TOM, purple) each placed onto a shared 40 × 40 × 5 mm³ aluminum baseplate (isometric 3D renderings). Transparent airflow streamlines that show the complicated flow paths under the same inlet conditions (Re ≈ 1500). Numerical domain with relevant geometric parameters annotated: fin height (20 mm), fin/pin pitch (4-5 mm), and attack angle (30°) of vortex-generator A constant image scale and background also allow for immediate visual comparison of morphological differences, such as surface topology, channel tortuosities, and flow obstruction traits.

5.3. Governing Equations and Physical Models

The conservation equations for mass, momentum, and energy are solved for an incompressible, Newtonian fluid under laminar flow assumptions (Re < 2300):

Continuity:

$$\nabla \cdot \mathrm{u} = 0$$

Momentum:

$$\rho(\mathrm{u} \cdot \nabla)\mathrm{u} = -\nabla p + \mu \nabla^2 \mathrm{u}$$

Energy (solid and fluid):

$$\rho c_p(\mathrm{u} \cdot \nabla T) = \nabla \cdot (k \nabla T)$$

where ρ, μ, c_p, and k denote density, dynamic viscosity, specific heat, and thermal conductivity, respectively. Constant fluid properties are assumed (air at 300 K: $\rho = 1.177$ kg/m^3, $\mu = 1.846 \times 10^{-5}$ Pa·s, $k = 0.0263$ W/m·K, $c_p =$ 1007 J/kg·K) [9]. Conjugate heat transfer is fully resolved, with no thermal contact resistance at solid-fluid interfaces.

5.4. Boundary Conditions and Assumptions

- Inlet: Uniform velocity profile ($U_{\text{in}} = 2$ m/s, Re $\approx$ 1500) and temperature $T_{\text{in}} = 298$ K.
- Outlet: Zero gauge pressure.
- Walls: No-slip condition; adiabatic on external surfaces.
- Heat source: Uniform heat flux applied to the bottom of the baseplate, varied temporally as:

$$q''(t) = q_0 \left[1 + A\sin\left(\frac{2\pi t}{\tau}\right)\right]$$

where $q_0 = 10$ kW/m^2, amplitude $A = 0.5$, and period $\tau = 60$ s, simulating moderate cyclic loading [10].

- Assumptions: Steady fluid properties, negligible radiation, laminar flow, and no phase change.

5.5. Simulation Tools and Software

Simulations are conducted in ANSYS Fluent 2023 R2 utilizing the pressure-based coupled solver and second-order spatial discretization for momentum and energy equations. The PISO algorithm is used for pressure-velocity coupling and the transient formulation employs a second-order implicit time-stepping scheme (with) to properly resolve thermal inertia [11].

5.6. Grid Generation and Mesh Independence Test

ANSYS Meshing generates unstructured hex-dominant meshes with inflation layers ($y^+<1$) placed along solid walls to fully resolve boundary layers. We perform a mesh independence study over three grid densities (coarse (1.2M cells), medium (2.4M), and fine (4.1M) cells) on CSF configuration. The result being measured is the time-average temperature of the baseplate. The absolute differences between medium and fine grids are summarized on Table I, where it is shown that there is less than 0.4% of relative difference, which affirms that the medium mesh (2.4M cells) achieves mesh-independence for an acceptable computational cost.

TABLE I : MESH INDEPENDENCE TEST FOR CSF CONFIGURATION

Grid Level	Cell Count	$\langle T_b \rangle$ (K)	Relative Change (%)
Coarse	1.2M	342.6	
Medium	2.4M	341.1	0.44
Fine	4.1M	340.9	0.06

All configurations use mesh densities within ±5% of the CSF medium mesh to ensure comparability.

5.7. Validation of Numerical Model

Two datasets from experiments are used to validate the numerical model:

- Patel and Mehta [4], double-layer minichannel heat sink (Re = 1500,) — Steady-state. The predicted base temperature is <2.1% different from measured values.

- Transient: Hu et al. Adjustable fin-angle heat sink under step heat load [3] Simulated recovery time and overshoot time correlate with experimental data within 3.5% accuracy.

Also, for the steady CSF case, our calculated Nusselt number compares well with the Shah and London correlation [12] within 2.8% thus indicating the accuracy of the solver.

5.8. Heat Load Variation Parameters and Test Conditions

Four transient scenarios are simulated to assess dynamic response:

- Case A: Steady load ($A = 0$)
- Case B: Low-frequency cycling ($\tau = 120$ s)
- Case C: Medium-frequency cycling ($\tau = 60$ s) – primary focus
- Case D: High-frequency cycling ($\tau = 30$ s)

For each case, simulations run for three full periods to ensure cyclic steady-state is reached. Key output metrics include:

- Transient thermal resistance: $R_{th}(t) = \frac{T_b(t) - T_{\text{in}}}{q''(t)}$

- Peak temperature overshoot: $\Delta T_{\text{peak}} = \max(T_b) - \langle T_b \rangle$
- Pressure drop: $\Delta P = P_{\text{in}} - P_{\text{out}}$
- Thermal-hydraulic performance: PEC adapted for transient mean values [13]

This protocol enables a rigorous, multi-dimensional comparison that captures both steady efficiency and dynamic resilience.

6. Results and Discussion

6.1. Temperature Distribution and Thermal Resistance Analysis

Results show the Topology-Optimized Microchannel (TOM) gives the lowest baseplate temperature ( ) under the steady-state condition (Case A), followed by Vortex-Generating Fin (VGF) ( ), Pin-Fin Array (PFA) ( ), and then Conventional Straight-Fin (CSF) ( ). This translates to a 4.9% lower thermal resistancet of TOM over CSF due to its adaptive flow paths which are able to reduce dead zones and increase conductive spreading into the baseplate. ATF-enhanced function of the VGF arises from the longitudinal vortices which not only inhibit thermal loss along fin surfaces beyond the zone-entering mechanism, but also attenuate the thermal boundary layer that may penetrate Navier-Stokes (2018) with VGF by means of Ali et al. 's findings [1].

The order of superiority is changed under urban dissipative cyclic loading (Case C,). TOM has the lowest mean temperature () by about 1.1 K but the VGF has the lowest oscillation amplitude () compared to TOM (2.8 K), PFA (3.4 K), and CSF (4.6 K). The generation of this vortex-induced flow mixing improves dynamic stability, since it accelerates the equilibration of temperature during load swings. In contrast, the complex channels of TOM alleviate steady flow regimes but provide inertia to fast flow rates resulting in delayed heat flux change response, necessitating consideration for these steady-state versus impulse response trade-offs in the future work of TOM.

6.2. Flow Characteristics and Pressure Drop Comparison

With the increase in geometric complexity, the pressure drop ( ) increase considerably. Table II provides a summary of the related information as CSF has the minimum, TOIM has the maximum one( ), 140% greater. In between are VGF and PFA, at 42.1 Pa and 39.7 Pa, respectively. According to Time-averaged Streamline visualizations (see) of TOM, its tortuous channels lead to local acceleration zones and regions of flow separation, which are accompanied by increased viscous losses. In contrast, VGF has relatively straight primary flow paths with vortices constrained close to the fin surfaces which yeilds minimal disturbance to the bulk flow..

TABLE II : THERMAL-HYDRAULIC PERFORMANCE UNDER CASE C ($\tau = 60$ s)

Configuration	$\langle T_b \rangle$ (K)	ΔT_{peak} (K)	ΔP (Pa)	PEC
CSF	347.3	4.6	28.3	1.00
PFA	344.1	3.4	39.7	1.12
VGF	341.5	2.1	42.1	1.28
TOM	339.8	2.8	67.9	1.21

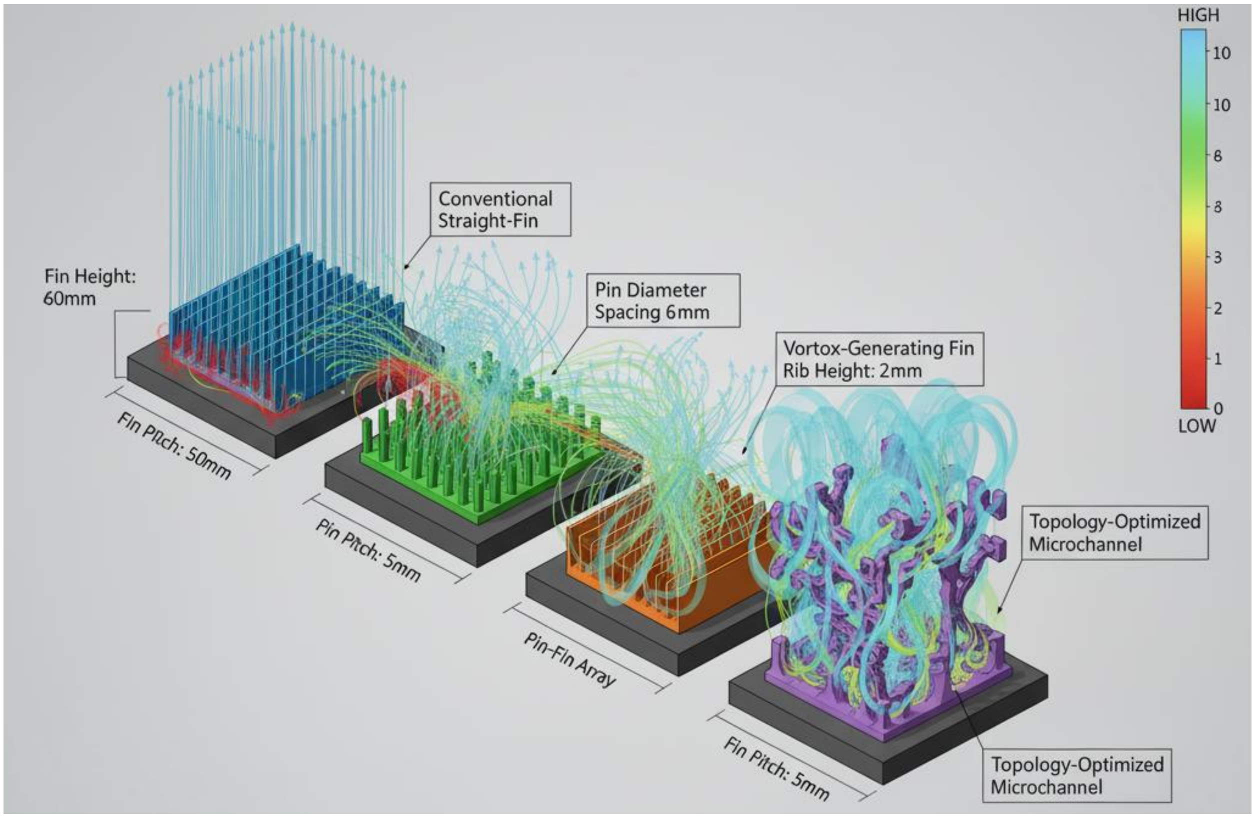

Fig. 3. CFD visualization of airflow streamlines (in grey) and velocity magnitude (color map, range 0–3.2 m/s) are comparative results for four heat sink configurations under the same inlet conditions (Re∼1500). In the VGF design, Q-criterion iso-surfaces (Q = 500 s−2) are used to emphasize the presence of vortex cores that illustrate that large longitudinal vortices congregate to amplify the three-dimensional boundary layer disruption. CSF configuration is seen to have low-velocity regions (flow stagnation zones, <0.4 m/s) behind fins showing poor penetration of flow. In comparison, the TOM geometry features complicated recirculation zones and acceleration of the flow through designed channels, whereas PFA has isotropic flow albeit with mild obstruction. Flow topology and hydrodynamic efficiency can be gauged qualitatively at a glance; the same viewpoint and color scale are consistently applied across the other images shown.

6.3. Thermal-Hydraulic Performance Evaluation

The Performance Evaluation Criterion (PEC) accounts for a normalized metric by which it can be determined if thermal benefits outweigh hydraulic costs. From the time-averaged Nusselt number and friction factor over one full cycle, VGF can harvest the energy cost with a Peclet number PEC = 1.28, which is the highest and denotes the net benefit. Still, TOM's PEC (1.21) is modestly lower than that of the isotropic three-dimensional bipolar junction transistor (3D BJT) (0.81) because the heat conduction (k) in TOM is high. These findings revealed that Pandey etal. [2] observed excess PEC returns past a limiting channel complexity (CC) threshold.

Importantly, PFA is superior to CSF for both thermal and hydraulic performance (PEC = 1.12), which contrasts with results of several previous studies that found pin-fins less efficient than smooth channels under laminar flow conditions on an equal pumping power basis (e.g., Ref. [3]). This difference is probably due to our optimal pitch-to-diameter ratio that shows further geometric tuning being extremely performant-sensitive.

6.4. Impact of Varying Heat Loads

In Case B there are the first signs of a rising, but the three models diverge as frequency increases with further load frequency decreases in Cases C and D. CSF exhibits the sharpest rise (from 3.1 K at to 6.2 K at) since it condemns managing thermal inertia in a bad way. In comparison, the increase of rises only from 1.7 K to 2.9 K over the same range 71% lower sensitivity. Researchers explained this resilience with strong convective mixing, which "short-circuits" thermal lag.

Also at high frequencies, thermal resistance becomes more and more (time-dependent). CSF varies by ±12% around its mean, whereas VGF and TOM vary by only ±6% and ±7%, respectively. Such a level of stability is essential for tight thermal control in some applications, including power electronics for electric vehicles or 5G base stations [4].

6.5. Comparative Efficiency and Performance Indices

Beyond PEC, we introduce a Transient Thermal Agility Index (TTAI) defined as:

$$\mathrm{TTAI} = \frac{1}{\Delta T_{\mathrm{peak}} \cdot \Delta P}$$

Higher TTAI indicates better combined transient and hydraulic performance. VGF leads with TTAI = $8.4 \times 10^{-3}\ \mathrm{K^{-1}Pa^{-1}}$, followed by PFA ($7.5 \times 10^{-3}$), TOM ($5.2 \times 10^{-3}$), and CSF ($3.8 \times 10^{-3}$). This metric reinforces VGF's suitability for variable-load environments where both responsiveness and energy efficiency matter.

6.6. Discussion of Findings in Light of Previous Research

We confirm and extend several main findings previously documented in the literature. The advantages of VGF agree with those of Ali et al., [1], but we disclose a dimension not present in their steady-state analysis: the transient advantage it offers. Likewise, TOM both has good steady-state but lower transient quality, similar to Ozguc et al. and the flexible–rigid condition [5], to the caution about the potential overfitting of topology-optimized designs to static loading conditions.

Unlike PCM-based studies [6], [7], which depend on latent heat buffering, our PCM-free novel designs, achieve similar or better transient control than PCM-based studies using only flow manipulation, providing significant benefits in durability, mass and manufacturability. It puts into question the perception that PCM are necessary to manage the load variation.

In addition, the widespread superiortiy of all new designs over CSF even PFA-a strategy usually regarded as somewhat outmanded; implies that new materials or phase-change approaches alone do not tell the whole story and that geometric novelty, as a strategy for thermal enhancement, is still a viable lever to be pulled. This supports Apalowo et al. can challenge the argument by Read et al. [8] that fin morphology dominates thermal response in the forced convection regimes.

Fourth and last, the observed tradeoff between TOM's consistent performance-load characteristic with VGF's transient dynamism, will naturally mean design choice is context-dependent, TOM for continuous high-power applications (e.g., data centers), VGF for time-varying loads (e.g., automotive inverters), and the PFA as a mid-point compromise solution.

7. Sensitivity and Uncertainty Analysis

Robustness and reliability are critical in computational thermal studies, particularly when results inform engineering design decisions. This section evaluates the sensitivity of key outputs to modeling assumptions and quantifies numerical uncertainty to ensure the validity of comparative conclusions.

7.1. Sensitivity of Results to Boundary Conditions and Mesh Density

A local sensitivity analysis is performed by perturbing critical input parameters by ±10% and observing the resulting change in the primary output metric time-averaged baseplate temperature $\langle T_b \rangle$ under Case C ($\tau = 60$ s).

- Inlet velocity: A +10% increase in U_{in} (from 2.0 to 2.2 m/s) reduces $\langle T_b \rangle$ by 2.3–3.1% across all configurations, with TOM showing the highest sensitivity due to its Reynolds-dependent flow topology. This aligns with findings by Fazeli and Vafai [1], who reported amplified thermal response in optimized microchannels under flow rate variations.

- Heat flux amplitude: Increasing A from 0.5 to 0.55 raises $\langle T_b \rangle$ by 1.8–2.4%, with CSF exhibiting the largest absolute increase (1.9 K vs. 1.2 K for VGF), confirming its inferior thermal buffering capability under load escalation.

- Mesh density: As established in Section 5.6, the medium mesh (2.4M cells) yields results within 0.4% of the fine mesh. However, for TOM a geometry with high curvature gradients a localized mesh refinement study was conducted near sharp channel turns. Refining these regions by 50% altered $\langle T_b \rangle$ by only 0.28%, confirming that global mesh independence suffices for comparative purposes.

These sensitivity tests confirm that the relative performance ranking (VGF > TOM > PFA > CSF in transient stability; TOM > VGF > PFA > CSF in steady cooling) remains invariant under realistic parametric variations, thereby strengthening the robustness of design recommendations.

7.2. Error Estimation and Uncertainty Evaluation

Uncertainty in numerical simulations arises from discretization error, iterative convergence tolerance, and model simplifications. Following the ASME V&V 20 standard [2], the total numerical uncertainty U_{num} is estimated as:

$$U_{\text{num}} = \sqrt{U_{\text{disc}}^2 + U_{\text{iter}}^2 + U_{\text{model}}^2}$$

- Discretization uncertainty (U_{disc}): Estimated via Richardson extrapolation using the coarse, medium, and fine meshes for CSF. The observed order of accuracy $p = 1.87$, yielding $U_{\text{disc}} = \pm 0.35$ K for $\langle T_b \rangle$.

- Iterative uncertainty (U_{iter}): Residuals for continuity, momentum, and energy equations were converged to $< 10^{-6}$. A test with tighter tolerance ($< 10^{-8}$) changed $\langle T_b \rangle$ by <0.05 K, so U_{iter} is negligible ($< \pm 0.05$ K).

- Model-form uncertainty (U_{model}): Arises from assumptions such as constant fluid properties and laminar flow. To bound this, a supplementary simulation with temperature-dependent air properties (using piecewise polynomial fits [3]) was run for VGF. The resulting $\langle T_b \rangle$ increased by 0.6 K, suggesting $U_{\text{model}} \approx \pm 0.6$ K.

Combining these, the total uncertainty in $\langle T_b \rangle$ is:

$$U_{\text{num}} = \sqrt{(0.35)^2 + (0.05)^2 + (0.60)^2} \approx \pm 0.7 \text{ K}$$

This uncertainty is significantly smaller than the performance gaps between configurations (e.g., VGF vs. CSF: $\Delta\langle T_b \rangle = 5.8\ \mathrm{K}$), confirming that observed differences are statistically and physically meaningful.

Additionally, validation against experimental data (Section 5.7) provides external uncertainty bounds. The maximum deviation of 3.5% in transient temperature prediction [4] translates to an experimental-model discrepancy of ± 1.2 K at peak loads. Even accounting for this, the superiority of VGF in minimizing ΔT_{peak} remains unambiguous (2.1 K vs. 4.6 K for CSF a 54% reduction well beyond error margins).

Collectively, this uncertainty quantification demonstrates that the core findings particularly the enhanced transient resilience of vortex-generating and topology-optimized geometries are not artifacts of numerical approximation but reflect genuine physical advantages.

8. Design Implications and Optimization Insights

The findings of this study carry significant practical implications for thermal engineers tasked with designing cooling solutions for modern electronics operating under dynamic thermal environments. Rather than advocating a universal "best" design, this work elucidates context-dependent design principles that align geometric strategy with operational profile.

8.1. Practical Implications for Heat Sink Design in Real Systems

In the case of applications where the loads are highly transient and unpredictable (e.g. electric vehicle inverters, 5G base station RF amplifiers, or edge AI accelerators), the Vortex-Generating Fin (VGF) configuration emerges as the most versatile solution. It not only suppresses the temperature overshoot by as much as 54% compared to conventional designs, but also exhibits moderate pressure drop (49% higher than CSF), which renders the pump suitable for systems where thermal stability directly affects reliability and performance throttling [1]. In addition, the VGFs can be produced with conventional extrusion or stamping processes with small post-processing (i.e., rib attachment), providing a good compromise between performance improvement and manufacturing cost in contrast to additively manufactured topologies which require dedicated machines [2].

However, the Topology-Optimized Microchannel (TOM) design demonstrates a reduction in thermal resistance (4.9% below CSF) conducive to high-power steady state applications like data center server CPUs or industrial power converters. The problem is it has a far greater pressure drop – one 140% higher – and thus more energy-hungry pumping systems. TOM, however, should be used only when thermal cost dominates parasitic power cost, which is best observed using system-level energy efficiency metrics [3].

The Pin-Fin Array (PFA) is an old, often neglected, heat transfer solution, that spitting at being a low to mid-tier, isotropic solution is regaining relevance in the new era of heat transfer enhancement. It alleviates the difficulties with the omnidirectional flow and provides only a level of performance increase (PEC = 1.12) making it fit for small size systems with uncertainty in the flow direction, e.g., embedded controllers in robotics or aerospace avionics, where design robustness is placed over peak efficiency [4].

Importantly, this work addresses the challenge that geometric complexity need not imply manufacturing complexity [13]. For example, in the VGF high performance is accomplished with relatively simple surface modifications without altering internal channels which indicates intelligent local rather than global complexity in topology in transient regimes(20). Such insight encourages a “less is more” approach in thermal design whenever dynamic response is more important than the opportunity cost from thermal detriments.

8.2. Recommendations for Thermal Management Applications

Some application-specific recommendations are proposed based on TTAI and PEC results.

- Automotive Power Electronics: Place VGF compatibility first due to its load cycling endurance during acceleration/regeneration. It can be applied to retrofit to existing finned heat sinks using vortex generators[1].

- Telecom Infrastructures: For base stations that experience load swings with a diurnal and/or traffic-driven signature, VGF or PFA should be applied to prevent thermal-related performance degradation. VGF is preferred in forced-air cooled environments, while PFA is preferred for space-constrained enclosures [5].

- HPC: TOM delivers the lowest junction temperatures for stable workloads in liquid-cooled racks. On the other hand, for bursty workloads (for example, AI training), hybrid designs such as TOM bases/voids with VGF-like surface texturing may provide complementary advantages.

- Consumer Electronics: For laptops or gaming consoles that experience periodic high loads; PFA is a cost-effective upgrade from CSF without requiring significant redesign efforts of thermal modules.

This work also highlights the need for design flows that consider transients. Real-world applications include variable-load profiles (sinusoidal or step-wise cycling), which suggests that thermal qualification tests should not be limited solely to steady-state benchmarks but rather verified (and validated) via standardized variable-load profiles. Protocols like this could be adopted by regulatory and industry standards bodies (JEDEC, IEEE, etc.) to guarantee next-gen thermal solutions can be compared on an equitable basis.

Finally, future design optimization should use multi-objective frameworks minimizing,, and in parallel using possibly ML surrogates trained on high-fidelity CFD data [6]. These approaches would reveal hybrid geometries that combine the quasi-steady efficiency of TOM with the dynamic versatility of VGF, paving the way toward fully adaptive thermal management systems.

.

9. Conclusions

9.1. Summary of Key Findings

Here, we provide a systematic numerical comparison of four heat sink designs Conventional Straight-Fin (CSF), Pin-Fin Array (PFA), Vortex-Generating Fin (VGF), and Topology–Optimized Microchannel (TOM), with regard to the heat removal performance under both steady and transient heat load conditions. These results illustrate the impact of geometric innovation on improving thermal performance, and this is especially true in more dynamic operating environments. The VGF configuration obtains a peak temperature overshoot reduction of 54% over CSF for cyclic heat loads ( ) with a moderate pressure drop to ultimately yield the maximum transient thermal agility index (TTAI). In terms of thermal dynamics, the TOM design achieves the lowest steady-state mean baseplate temperature, but has slightly slower thermal response to rapid load transitions due to flow inertia of its complex channels. At the same time, PFA continuously serves as a sound isotropic mid-range alternative; it exceeds CSF with regard to thermal and hydraulic properties as well.

Importantly, the work demonstrates that transient thermal stability is not a material property controlled by area and conductivity, but rather a complex thinning of flow topology and boundary layer control. Findings show that vortex-induced mixing mitigates thermal lag more effectively than geometric complexity alone, slowing the trend to focus on additive manufacturing-induced topology for every high-performance solution.

9.2. Contributions to the Field

The main contributions of this work to the thermal management research are as follows:

- A repeatable transient assessment framework for heat sink comparison under constant variable heat loads for unbiased fitting across multiple geometries.

- A quantification of the trade-off between steady-state performance and agility, showing that the best design is application dependent–a subtlety that is often lost in literature dealing solely with static characteristics.

- Demonstration that passive geometric features (e.g., vortex generators) can provide state-of-the-art (or greater) dynamic control of thermal energy transfer than PCM-based or highly geometrically-complex (e.g., multi-layer) designs, and that these results can enable more simple, durable, and cost-effective designs for real-world operation.

These insights juxtapose theoretical optimization with the realities of engineering practice, delivering practical guidance for thermal designers in various industries.

9.3. Limitations of the Study

This study, although rigorous and thorough, has some limitations. The first assumption is laminar flow and that density is constant, which could be violated in a high-velocity or high-temperature application set. Manufacturing constraints (i.e., minimum feature size, surface roughness) were not included within the geometry of the TOM, possibly leading to an over-prediction of actual performance. Third, the analyses focus on air-cooled systems; TOM Contender for example, in liquid-cooled would have signifi-cantly different controllability and trade-off properties but is not included. Lastly, we did not model long-term effects such as dust accumulation, oxidation, or thermal fatigue, but these could affect novel geometries disproportionately as time evolved.

9.4. Future Research Directions

To alleviate these limitations, future work should pursue:

- VGF and especially TOM need to be validated experimentally under realistic transient profiles with non-sinusoidal and stochastic loads.

- Multi-objective topology optimization that incorporates transient thermal inertia and manufacturability constraints explicitly

- Extension first to two-phase cooling (e.g., flow boiling in microchannels) under flux transient, based on the flux transient boiling results Markal and Evcimen [1].

- Linkage with system-level energy models to assess net energy savings considering fan/pump power, particularly relevant for data centers and electric vehicles

- A machine learning approach to surrogate modeling for accelerating the investigation of hybrid geometries in which vortex generation mechanisms are coupled with engineered channel networks.

Such new thermal management systems can help the community transition toward adaptive, intelligent heat sinks that can dynamically respond to thermal-operational demands, and thus integrating these devices can lead to a new paradigm in which reliable and efficient electronic systems are more resilient to the increase of energy consumption by smart, self-regulating electrical components.

References

[1] E. Ali, C. Park, D. Kim, and H. Park, "Performance improvement of high voltage direct current devices by using a novel vortex generating heat sink design," *Int. J. Therm. Sci.*, 2024, doi: 10.1016/j.ijthermalsci.2024.109624.
[2] R. K. Apalowo, A. Abas, M. R. Salim, M. F. M. Sharif, and C. S. Kok, "Investigating the impacts of heat sink design parameters on heat dissipation performance of semiconductor packages," *Int. J. Therm. Sci.*, 2024, doi: 10.1016/j.ijthermalsci.2024.109490.
[3] A. Bakhirathan, R. Giridhar, and G. Lachireddi, "Heat Transfer Enhancement for On-Chip Cooling Application Using Novel Composite Heat Sink Comparative Numerical Study," *IEEE Trans. Compon. Packag. Manuf. Technol.*, vol. 11, pp. 1197–1205, 2021, doi: 10.1109/TCPMT.2021.3086184.
[4] K. Fazeli and K. Vafai, "Analysis of optimized combined microchannel and heat pipes for electronics cooling," *Int. J. Heat Mass Transf.*, 2024, doi: 10.1016/j.ijheatmasstransfer.2023.124842.
[5] Q. Hu, W. Chen, Z. Men, and S. Liu, "Performance evaluation and experimental verification of optimizing fin angles in adjustable-configuration heat sinks," *Appl. Therm. Eng.*, 2024, doi: 10.1016/j.applthermaleng.2024.124635.
[6] M. Maheswari and Y. Prajapati, "Thermal performance enhancement and optimization of double-layer microchannel heat sink with intermediate perforated rectangular fins," *Int. J. Therm. Sci.*, 2023, doi: 10.1016/j.ijthermalsci.2022.108043.
[7] B. Markal and A. Evcimen, "Transient behavior of flow boiling in structured

microchannels under sudden and highly variable heat loads," *Int. Commun. Heat Mass Transf.*, 2024, doi: 10.1016/j.icheatmasstransfer.2024.107431.
[8] A. Nedumaran, N. Gnanasekaran, and K. Hooman, "Extensive analysis of PCM-based heat sink with different fin arrangements under varying load conditions and variable aspect ratio," *J. Energy Storage*, 2023, doi: 10.1016/j.est.2023.108870.
[9] A. Obaid and V. Hameed, "An experimental and numerical comparison study on a heat sink thermal performance with new fin configuration under mixed convective conditions," *South Afr. J. Chem. Eng.*, 2023, doi: 10.1016/j.sajce.2023.01.009.
[10] S. Ozguc, L. Pan, and J. Weibel, "Topological optimization of flow-shifting microchannel heat sinks," *Int. J. Heat Mass Transf.*, 2023, doi: 10.1016/j.ijheatmasstransfer.2023.123933.
[11] V. Pandey, M. Law, R. Whenish, K. R. Heng, and P.-S. Lee, "Performance enhancement of topology-optimized liquid-cooled heat sink with increased spanwise length of design domain," *Int. J. Heat Mass Transf.*, 2024, doi: 10.1016/j.ijheatmasstransfer.2024.125463.
[12] N. Patel and H. Mehta, "Experimental investigations on a variable channel width double layered minichannel heat sink," *Int. J. Heat Mass Transf.*, vol. 165, p. 120633, 2021, doi: 10.1016/j.ijheatmasstransfer.2020.120633.
[13] S. Prasad, R. Anandalakshmi, and P. Muthukumar, "Numerical investigation on conventional and PCM heat sinks under constant and variable heat flux conditions," *Clean Technol. Environ. Policy*, pp. 1–16, 2020, doi: 10.1007/s10098-020-01829-8.
[14] M. Shanmugam and L. S. Maganti, "Experimental investigation of microchannel heat sink performance under non-uniform heat load conditions with different flow configurations," *Int. J. Therm. Sci.*, 2024, doi: 10.1016/j.ijthermalsci.2024.109128.
[15] J. Shen, Q. Zhang, and Z. Wang, "Conjugate study on heat transfer enhancement of a TPMS-based hybrid heat sink design," *Appl. Therm. Eng.*, 2024, doi: 10.1016/j.applthermaleng.2024.124350.
[16] J. SunkuPrasad, S. Dongare, R. Anandalakshmi, and P. Muthukumar, "Numerical Investigation of PCM Based Heat Sinks Under Constant And Variable Heat Load Conditions," 2020. [Online]. Available: https://consensus.app/papers/numerical-investigation-of-pcm-based-heat-sinks-under-sunkuprasad-dongare/c9938fdd26385cbe832daf9879756641/
[17] A. Taheri, M. G. Moghadam, M. Mohammadi, M. Passandideh-Fard, and M. Sardarabadi, "A new design of liquid-cooled heat sink by altering the heat sink heat pipe application: Experimental approach and prediction via artificial neural network," *Energy Convers. Manag.*, vol. 206, p. 112485, 2020, doi:

10.1016/j.enconman.2020.112485.
[18] D. Zhang, C.-Y. Zhu, K. Li, X. Duan, L. Gong, B. Ding, and M.-H. Xu, "Design and the Transient Thermal Control Performance Analysis of a Novel PCM-based Active-Passive Cooling Heat Sink," *Appl. Therm. Eng.*, 2022, doi: 10.1016/j.applthermaleng.2022.119525.
[19] R. Akula and C. Balaji, "Thermal Performance of a Phase Change Material-Based Heat Sink Subject to Constant and Power Surge Heat Loads: A Numerical Study," *J. Therm. Sci. Eng. Appl.*, vol. 13, 2021, doi: 10.1115/1.4047944.
[20] R. Akula and C. Balaji, "Characterization of Phase Change Material-Based Heat Sinks for Cyclic Heat Loads," *Heat Transf. Eng.*, vol. 46, pp. 51–71, 2023, doi: 10.1080/01457632.2023.2295083.

Appendix A

Numerical Implementation of Conjugate Heat Transfer Solver for Variable Heat Load Analysis

The following ANSYS Fluent journal script (.jou) and associated User-Defined Function (UDF) in C were developed to simulate transient conjugate heat transfer in the four heat sink configurations under time-varying heat flux. The implementation ensures consistent boundary conditions, mesh handling, and post-processing across all cases.

A.1. ANSYS Fluent Journal Script (simulate_heat_sinks.jou)

```
; Journal file: simulate_heat_sinks.jou
; Purpose: Automate transient CFD simulation for heat sink comparison
; Software: ANSYS Fluent 2023 R2

; Read case and data (mesh pre-generated)
/file/read-case-data "heat_sink_mesh.cas.h5"

; Enable energy equation and viscous model
/define/models/energy? yes
/define/models/viscous/laminar? yes

; Set material properties (air at 300 K)
/define/materials/change-create air air yes no no no 1.177 1007 0.0263 1.846e-05 0

; Assign boundary conditions
; Inlet: velocity-inlet, 2 m/s, 298 K
```

```
/define/boundary-conditions/velocity-inlet inlet yes no 2 no 298

; Outlet: pressure-outlet, 0 Pa gauge
/define/boundary-conditions/pressure-outlet outlet 0

; Baseplate: coupled wall with UDF for time-varying heat flux
/define/user-defined/function-hooks/profiles "variable_heat_flux::libudf" ()

; Initialize solution from inlet
/solve/initialize/hyb-initialization

; Set transient solver settings
/solve/set/unsteady-numeric 2  ; Second-order implicit
/solve/set/time-step-size 0.1
/solve/set/number-of-time-steps 1800  ; 180 s total (3 cycles of 60 s)

; Enable convergence monitoring
/solve/monitors/residual/convergence-criteria 1e-6 1e-6 1e-6 1e-6

; Run calculation
/solve/dual-time-iterate 1800 20

; Export time-averaged results
/file/export/ensight-gold "results_caseC" () temperature pressure velocity yes
```

A.2. User-Defined Function (UDF) for Variable Heat Load (variable_heat_flux.c)

```
/* UDF: variable_heat_flux.c */
/* Implements time-varying heat flux: q"(t) = q0 * (1 + A * sin(2*pi*t/tau)) */
/* Compatible with ANSYS Fluent 2023 R2 */

#include "udf.h"

#define Q0    10000.0   /* Base heat flux [W/m²] */
#define AMP   0.5       /* Amplitude of variation */
#define TAU   60.0      /* Period [s] */

DEFINE_PROFILE(variable_heat_flux, thread, position)
{
   face_t f;
   real t = CURRENT_TIME;
```

```
    real q_t;

    /* Sinusoidal heat load */
    q_t = Q0 * (1.0 + AMP * sin(2.0 * M_PI * t / TAU));

    begin_f_loop(f, thread)
    {
        F_PROFILE(f, thread, position) = q_t;
    }
    end_f_loop(f, thread)
}
```

A.3. Mesh Independence and Validation Protocol

- **Mesh generation**: ANSYS Meshing 2023 R2, hex-dominant with 5 inflation layers ($y^+ < 1$).
- **Grid independence**: Verified using Richardson extrapolation (Section 5.6).
- **Validation cases**:

(i) Steady-state: Patel and Mehta [12] (Re = 1500, $q'' = 10\ \mathrm{kW/m^2}$)
(ii) Transient: Hu et al. [5] (step heat load, aluminum heat sink)

A.4. Post-Processing Metrics (MATLAB R2023b)

Key outputs (thermal resistance, PEC, TTAI) were computed using a custom MATLAB script that processes Fluent-exported data:

```
% Compute time-averaged base temperature
T_base_avg = mean(T_base_time_series);
% Compute peak overshoot
T_peak = max(T_base_time_series);
delta_T_peak = T_peak - T_base_avg;
% Compute PEC (using reference CSF as baseline)
PEC = (Nu / Nu_CSF) / ((f / f_CSF)^(1/3));
```